Available online at www.sciencedirect.com
SCIENCE DIRECT®
International Journal of Heat and Fluid Flow 25 (2004) 140–148
International Journal of HEAT AND FLUID FLOW
www.elsevier.com/locate/ijhff

Evaluation of heat and mass transfer phenomena in nucleate boiling

Peter Stephan, Jürgen Kern *

Darmstadt University of Technology, Chair of Technical Thermodynamics, Petersenstrasse 30, 64287 Darmstadt, Germany

Abstract

Based on experimental and theoretical investigations the present paper evaluates heat and mass transfer phenomena in nucleate boiling of pure substances and binary mixtures. It is recognized that microscale phenomena can be very important for the understanding and prediction of macroscopic heat transfer. Modeling strategies are presented that include microscale heat and mass transfer. The nucleate boiling heat transfer coefficient can be well predicted using these models and the process can be better explained taking the microscale phenomena into account. Microscale evaporation experiments of the authors confirm the modeling results on this scale. On the microscale, governing phenomena are: intermolecular forces of adsorption, capillary forces, molecular interfacial phase change resistance, and change of phase equilibrium. In a binary mixture, the phase equilibrium temperature is influenced by the strong gradient of concentration and thus the microscale heat transfer is significantly reduced. The contributions of diffusive mass transfer and variable thermophysical properties are negligible in microscale heat and mass transfer. On the macroscale, the influence of free and forced convection, transient heat conduction, and latent heat depends on the geometry of the evaporator and the boiling conditions. In a binary mixture, parameters are identified that are responsible for the characteristic reduction of heat transfer coefficients at intermediate mole fractions.
© 2003 Elsevier Inc. All rights reserved.

Keywords: Nucleate boiling; Heat transfer; Transport phenomena; Thin films; Binary mixtures

1. Introduction

For the design of nucleate boiling heat transfer devices often correlations are used to predict heat transfer coefficients. However, the accuracy of correlations is limited to the range of parameters they were developed for. The main reason for this restriction is the fact that correlations do not describe the governing physical phenomena in a comprehensive manner.

On a general point of view heat is transferred by free and forced convection, transient heat conduction, and latent heat. Bubbles grow and rise from a thin superheated liquid layer above the heated wall (Fig. 1). Due to the recent progress in the development of numerical models for the description of heat and mass transfer in boiling heat transfer as well as increasing computing capabilities, an identification of governing physical phenomena in nucleate boiling becomes possible. New measurement techniques towards smaller scales offer the possibility for a more detailed investigation of the mechanisms involved with the nucleate boiling process.

The aim of the present paper is to review the state of the art of understanding and modeling nucleate boiling heat and mass transfer of pure substances and binary mixtures. From that the predominant phenomena are derived and discussed. The results can be used in future works for facilitating the development of new models and correlations in order to achieve more reliable predictions.

In the first part of the paper, recent experimental and theoretical investigations are summarized that support the evaluation of heat and mass transfer phenomena in nucleate boiling. Based on a modeling theory that was developed by the authors, and verified by comparison of measured with computed heat transfer coefficients, the second part is dedicated to the identification of governing heat and mass transfer phenomena in nucleate boiling of pure substances and binary liquid mixtures.

2. Excerpt of experimental and theoretical investigations

This section gives a review of recent theoretical models and experimental investigations that concentrate

* Corresponding author. Tel.: +49-6151-16-6556; fax: +49-6151-16-6561.
E-mail address: jkern@ttd.tu-darmstadt.de (J. Kern).

0142-727X/$ - see front matter © 2003 Elsevier Inc. All rights reserved.
doi:10.1016/j.ijheatfluidflow.2003.11.006

Nomenclature

d	diameter (m)
$\dot{J}$	diffusive mass flow (kg/s)
l_o	characteristic length (m)
$\dot{M}$	convective mass flow (kg/s)
N_b	bubble site density (1/cm^2)
p	pressure (N/m^2)
p_c	critical pressure (N/m^2)
p_r	reduced pressure p/p_c (–)
$\dot{q}$	heat flux (W/m^2)
$\dot{Q}$	heat flow (W)
r	radius (m)
t	time (s)
t_o	reference time (s)
T	temperature (K)
ΔT	wall superheat (K)
x	mole fraction (–)
y	mass fraction (–)
y	coordinate normal to the wall (m)

Greeks

α	heat transfer coefficient (W/m^2 K)
δ	film thickness (m)
δ_w	wall thickness (m)
δ_{th}	thermal boundary layer thickness (m)
η	coordinate normal to the wall (m)
φ_{app}	apparent contact angle (–)
ξ	coordinate parallel to the wall (m)

Subscripts

ads	adsorbed
bulk	bulk
dep	departure
id	ideal
l	liquid
m	mean value
mic	micro-region
out	outer surface of the wall
sat	saturation
sub	subsystem
v	vapor
1	more volatile component

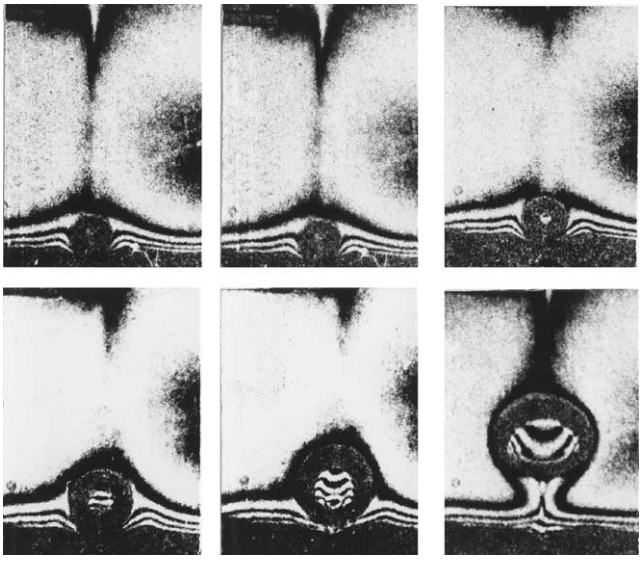

Fig. 1. Interferometric pattern around a growing and rising vapor bubble (Beer, 1971).

on, or can be used for, the evaluation of heat and mass transfer phenomena in nucleate boiling.

2.1. Experimental investigations

Based on experimental investigations (e.g., Forster and Zuber, 1954 as well as Hsu and Graham, 1961) the convective heat transfer is divided into free convection, enhanced forced convection around the site caused by the bubble motion during growth, and enhanced convection when the departing bubble's volume is replaced by bulk liquid.

Ammermann et al. (1996) determined experimentally the contributions of latent heat, natural convection, Marangoni flow, enhanced forced convection, and micro-convection to the total heat flux. Micro-convection accounts for the fact that superheated liquid surrounding the heated wire is entrained in the bubble wake (see Fig. 1). Evaporation (latent heat) was identified as the dominant mechanism (Fig. 2).

Judd and Hwang (1976) investigated experimentally boiling of dichlormethane on a glass surface using laser interferometry and high-speed photography. The results were used to support a model for predicting boiling heat flux incorporating micro-layer evaporation, natural convection, and nucleate boiling mechanisms. Micro-layer evaporation turned out to represent a significant proportion of the total heat transfer.

Bae et al. (1999) measured space- and time-resolved heat transfer variations during nucleate pool boiling of FC-72 using a microscale heater array in conjunction with a high-speed CCD camera. They also found that the major heat transfer mechanism is evaporation of liquid near the contact line. But heat transfer is highest during the departure process from the time the contact line reaches the maximum radial position to the departure time.

Höhmann and Stephan (2002) measured the wall temperature distribution close to the so-called

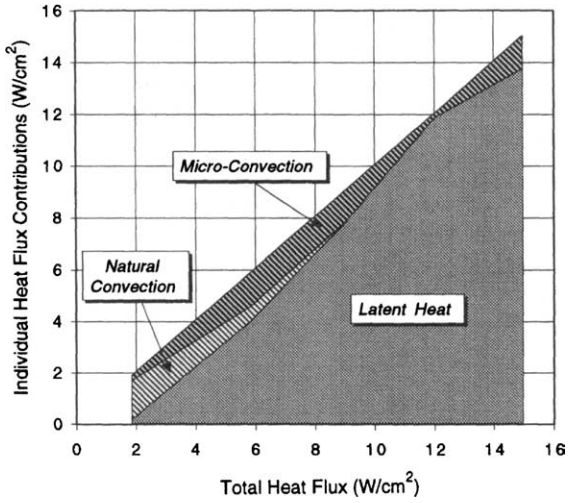

Fig. 2. Heat flux contributions for fully developed nucleate boiling of FC-72 on a heated wire (Ammermann et al., 1996).

micro-region where the liquid–vapor phase interface approaches the heated wall. With their capillary slot experiment, featuring an optical method using thermochromic liquid crystals (TLC), a strong temperature drop underneath the micro-region was observed indicating very high heat fluxes in the micro-region (Fig. 3). The left hand side of the temperature plot corresponds to the convection region in the fluid bulk (macro-region). Adjacent to this section with a constant temperature, the local cooling due to the high evaporation rate in the micro-region causes a strong temperature drop in the wall at the micro-region. The temperature then rises to a higher value, as the heat transfer in the adsorbed film region is small. The measured temperature data qualitatively agree well with the temperature distribution calculated by a micro-region model (Stephan et al., 2002) that represents the basis of the theoretical investigation described in the following section.

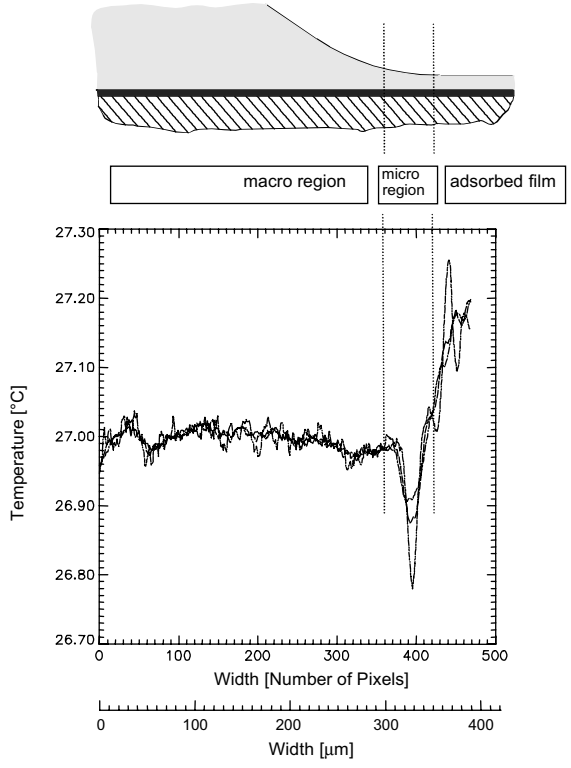

Fig. 3. Temperature distribution at the micro-region for evaporation of water at atmospheric pressure into air, different temperature plots indicate different types of spatial filters applied to the data of the TLC (Höhmann and Stephan, 2002).

2.2. Theoretical investigations

In the last decade, theoretical models have been developed for partial and fully developed nucleate boiling of pure substances. Fundamentally, they are all based on a thin film evaporation concept of Wayner et al. (1976). They investigated the evaporation of a liquid meniscus in a tiny area where the liquid–vapor interface approaches the wall (micro-region). In spite of the small geometrical dimensions (about one micrometer), a considerable amount of the supplied heat at the evaporator wall flows through the micro-region. In this region, microscale effects such as adhesion forces and interfacial thermal resistance in combination with a strong curvature change of the phase interface significantly influence local heat and mass transfer.

Stephan and Busse (1992) introduced a model to describe the heat and mass transfer in the micro-region and combined it with a macroscopic model for heat pipes. Good agreement with measured heat transfer data was found. To calculate the nucleate boiling heat transfer coefficient of pure substances, the micro-region model was implemented in a macroscopic vapor bubble growth model by several authors using different assumptions and simplifications (e.g., Dhir, 2001; Mann and Stephan, 2000a, Bai and Fujita, 1999).

Stephan and Hammer (1994) as well as Kern and Stephan (2000) developed a theoretical model for nucleate boiling heat transfer of pure substances and binary mixtures including the mentioned micro-region model. It is based on the assumption that the boiling system can be divided into small, symmetric subsystems, each of them containing a spherical vapor bubble. On the upper part of Fig. 4 the single bubble subsystem is shown. The diameter of the system d_{sub} depends on the active bubble site density. Boundary conditions are the saturation temperature T_{sat} and the outside wall temperature T_{out}, where δ_{th} is the thickness of the thermal boundary layer and δ_w denotes for the position of the thermocouples underneath the boiler surface in experiments. In order to calculate the heat flux, the computational domain is subdivided into two regions: the micro-region, where the liquid–vapor phase interphase approaches the wall, and the liquid adjacent to the

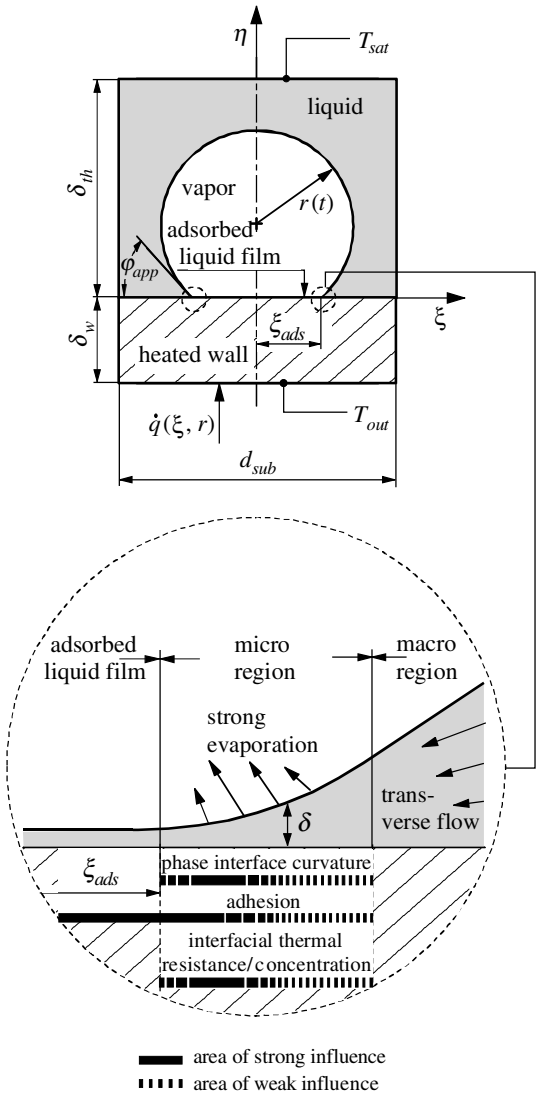

Fig. 4. Single bubble subsystem and significant phenomena in the micro-region.

micro-region as well as the wall, called macro region (see Fig. 4). Transport phenomena within the vapor bubble are insignificant for overall heat transfer coefficients (Krupiczka et al., 2000). Therefore the vapor is not included into one of these regions. The model accounts for a detailed description of microscopic and macroscopic transport phenomena. A numerical computation of the modeling equations yields the heat flux $\dot{q}(\xi, r)$ as well as the time depended radius of the vapor bubble $r(t)$. Further results are the apparent contact angle $\varphi_{\text{app}}(r)$ as well as the length ξ_{ads} of the adsorbed liquid film which covers the whole wall underneath the vapor bubble. The heat flux $\dot{q}(\xi, r)$ for the time period when the bubble is growing from an infinitesimal size to the departure radius then is averaged with respect to the heater area and the bubble growth time. Thereby the mean heat transfer coefficient is obtained:

$$\alpha_{\text{m}} = \frac{\dot{q}_{\text{m}}}{T_{\text{out}} - T_{\text{sat}}} \tag{1}$$

2.3. Verification of modeling theories

The presented model of Stephan and Hammer (1994) was used to calculate nucleate boiling heat transfer coefficients of different fluid wall combinations at various heat fluxes and vapor pressures (Hammer, 1996). Fig. 5 compares the results of the model with experimental data of Barthau (1992) and results from a correlation of Stephan and Abdelsalam (1980) for nucleate boiling of R114 on a copper plate. The deviation between numerical and experimental values is less than ±8%. The model has also been applied to further fluid wall combinations, e.g., boiling of water on a copper plate (Hammer and Stephan, 1995).

Computational results obtained with the presented model of Kern and Stephan (2000) for binary liquid mixtures are also in good agreement with data from experiments of Bednar and Bier (1994). The corresponding heat transfer coefficients are shown in Fig. 6. The error of measurement is in the range of ±10%. Furthermore values of frequently used correlations are plotted in that figure. The correlations of Fujita and Tsutsui (1994), Schlünder (1986), and Stephan and Körner (1969) also allow to calculate the heat transfer coefficient of binary mixtures, but only if the heat transfer coefficients of the two pure components are known. However, their correlations are partly based on different physical phenomena. Stephan and Körner take into account the local difference between liquid and vapor composition. Fujita and Tsutsui additionally consider the temperature difference between boiling and dew point curve at constant liquid concentration. Schlünder adds a diffusive mass transfer resistance in the near wall liquid layer.

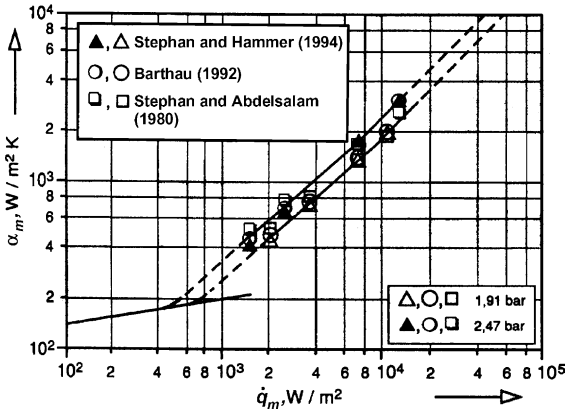

Fig. 5. Comparison of computational results with data from experiments (Barthau, 1992) and a correlation (Stephan and Abdelsalam, 1980) for boiling of the refrigerant R114 on a copper plate.

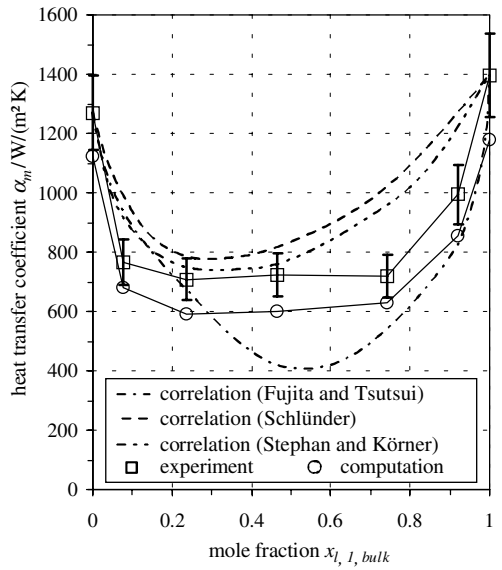

Fig. 6. Comparison of computational results (Kern and Stephan, 2003b) with data from experiments (Bednar and Bier, 1994) and correlations (Fujita and Tsutsui, 1994; Schlünder, 1986; and Stephan and Körner, 1969) of the binary mixture ethane/propane for different compositions, $p_r = 0.1$, $\dot{q}_m = 4 \times 10^3$ W/m^2.

Calculated heat transfer coefficients for pure substances and binary mixtures are almost always lower than measured heat transfer coefficients. This might result from the fact that the enhanced convection when the departing bubble's volume is replaced by bulk liquid is not yet included in the model. To account for enhanced convection, Dhir (2001) and co-workers developed a macro region model to calculate heat and mass transfer as well as the bubble shape of growing, departing, and rising vapor bubbles. Combining this macro region model with a micro-region model, they were able to compute heat transfer during the whole bubble growth cycle (Fig. 7). The model was verified by comparing computed with measured bubble shapes.

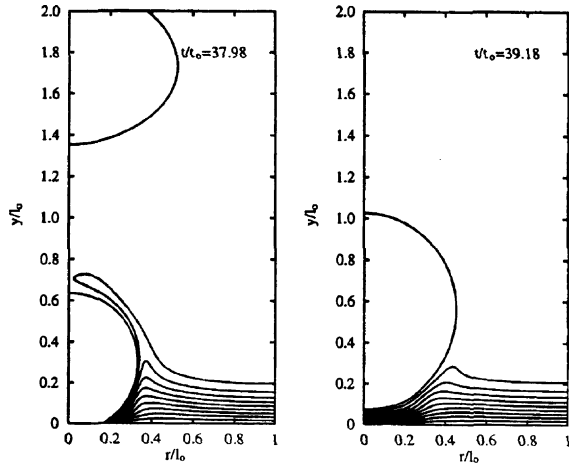

Fig. 7. Calculated isotherms of a single growing and departing vapor bubble at different points in time, boiling of water at atmospheric pressure (Dhir, 2001).

3. Governing transport phenomena

Despite of a lot of publications and discussions on nucleate boiling of pure substances and binary mixtures, it is still not clarified which transport phenomena govern the heat and mass transfer process. In this section governing transport phenomena in nucleate boiling heat transfer are identified. The studies are mainly based on a theoretical model that was developed by Stephan and Hammer (1994) as well as Kern and Stephan (2000, 2003a,b). Due to the separation of scales, the model distinguishes between microscopic and macroscopic transport phenomena.

3.1. Microscopic scale

If the thermal conductivity of the liquid is much smaller than that of the wall material, a significant part of the supplied heat at the evaporator wall flows through the micro-region (Fig. 4) where the thermal resistance of the liquid film with a thickness δ is small (Fig. 4). Therefore heat and mass transfer phenomena in the micro-region also govern overall heat transfer performance. Fig. 8 shows liquid film thickness and heat flux calculated in the micro-region of a binary mixture. Results for pure substances are qualitatively similar (Stephan and Hammer, 1994). Whereas in the macro region the phase interphase has a constant curvature corresponding to the bubble radius, in the micro-region the phase interphase curvature varies strongly (Fig. 8). The heat flux increases with decreasing film thickness and close to the adsorbed film the volatility is reduced by the adhesion pressure. The high local evaporation rate induces a transverse liquid flow into the micro-region. The pressure drop is driven by the phase interface curvature

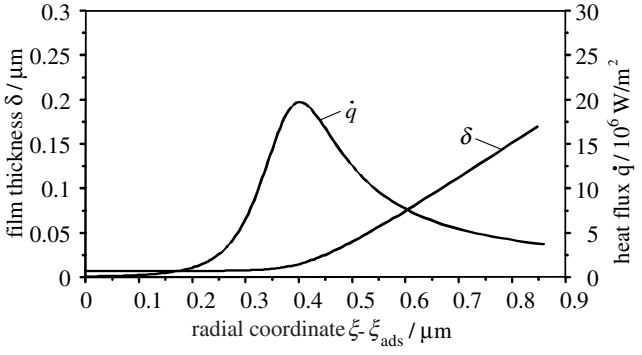

Fig. 8. Liquid film thickness and heat flux in the micro-region of the binary mixture propane/*n*-butane, $y_{l,l,bulk} = 0.063$, $p_r = 0.2$, $T_{out} - T_{sat} = 7,87$ K, $\xi_{ads} = 0.016$ mm, $r = 0.05$ mm.

effect and the adhesion effect. Their spheres of influence are schematically indicated in Fig. 4. The interfacial thermal resistance is important in the central part of the micro-region, because of the low thermal resistance of the thin liquid film and the high heat flux.

In a binary mixture one observes a preferential evaporation of one component of the mixture. Thus the concentration of this component decreases in the direction of the transverse liquid flow into the micro-region. As an example the mass fraction of the more volatile component propane in the liquid and vapor phase of the binary mixture propane/n-butane as a function of the radial coordinate are plotted in Fig. 9.

Due to this strong variation of concentration in the micro-region the following mixture effects caused by concentration gradients are considered in the model:

- diffusive mass transfer;
- Marangoni convection due to surface tension gradients;
- change of properties with concentration in general (e.g., density, viscosity, thermal conductivity, and latent heat of evaporation);
- change of equilibrium phase interface temperature (see saturation temperature in Fig. 9).

To evaluate mixture effects in the micro-region, our attention is drawn to a propane/*n*-butane mixture ($y_{l,1,\mathrm{bulk}} = 0.063$, $p_r = 0.2$, $T_{\mathrm{out}} - T_{\mathrm{sat}} = 7.87$ K). The saturation temperature amounts to $T_{\mathrm{sat}} = 335.45$ K and the radius of the single bubble at a certain point in time is $r = 0.05$ mm. An apparent contact angle of $\varphi_{\mathrm{app}} = 21.4°$ and an adsorbed film length of $\xi_{\mathrm{ads}} = 0.016$ mm are computed (see Fig. 4). The differential equations of the micro-region model are based on a scale analysis of the conservation equations. This analysis implies some simplifications (Kern and Stephan, 2003a). One of them reads that diffusive mass transfer normal to the wall, i.e., in η-direction (Fig. 4) can be neglected. To evaluate

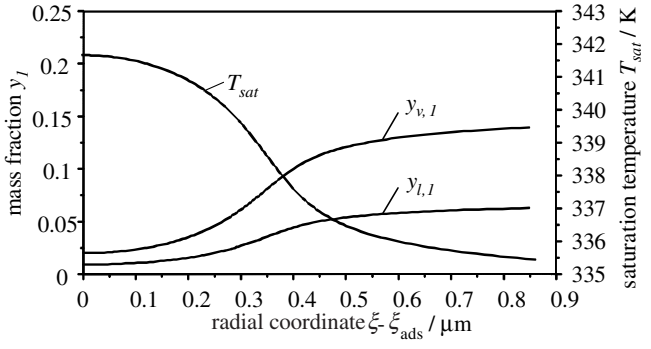

Fig. 9. Liquid and vapor mass fraction of the more volatile component propane as well as saturation temperature in the micro-region of the binary mixture propane/*n*-butane, conditions as for Fig. 8.

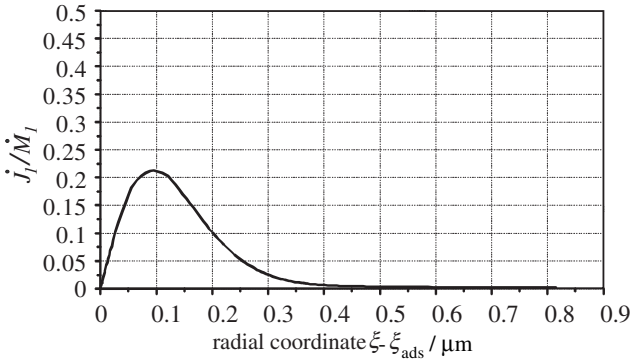

Fig. 10. Ratio of diffusive to convective mass flow of the more volatile component propane in the micro-region of the binary mixture propane/*n*-butane, $y_{l,1,\mathrm{bulk}} = 0.063$, $p_r = 0.2$, $T_{\mathrm{out}} - T_{\mathrm{sat}} = 7,87$ K, $\xi_{\mathrm{ads}} = 0.016$ mm, $r = 0.05$ mm.

diffusive mass transfer in radial direction (ξ) the calculated ratio of diffusive to convective mass flow of the more volatile component propane $\dot{J}_1/\dot{M}_1$ in the micro-region is shown in Fig. 10. Diffusion contributes with 5–20% to mass transfer where $0 \leqslant \xi - \xi_{\mathrm{ads}} \leqslant 0.25 \times 10^{-6}$ m, but only a very small amount of the heat flow passes through this area (see Fig. 8). For increasing values of $\xi - \xi_{\mathrm{ads}}$ the diffusive contribution tends to 0%. Therefore diffusive mass transfer is a negligible phenomenon in the micro-region.

The influence of further mixture effects on heat transfer in the micro-region is determined by parameter studies. In these computations all mixture effects are switched off except for, e.g., the variation of the saturation temperature with the concentration, i.e., no Marangoni convection is considered and the thermophysical properties are set constant corresponding to the values at bulk mole fraction $x_{\mathrm{l,bulk}}$ in the macro region. The heat flow in the micro-region $\dot{Q}_{\mathrm{mic}}$ that is calculated with these assumptions then is compared to the heat flow in the micro-region $\dot{Q}_{\mathrm{mic}}$ ($x_l = \mathrm{const.}$) without considering any mixture effects at all, i.e., concentration x_l is set constant. Fig. 11 shows that the ratio of these heat flows is about 0.7 for the mixture at different bulk compositions (rectangles in Fig. 11), i.e., the increase of the saturation temperature towards the bubble center leads to a decrease of heat transfer in the micro-region of about 30%. To compare this effect to the other two mixture effects, i.e., change of properties and Marangoni convection, the heat flow in the micro-region is computed assuming that the change of concentration leads to Marangoni convection only (rhombi in Fig. 11) or a variation of thermophysical properties only (triangles in Fig. 11), respectively. But these two mixture effects alter heat transfer in the micro-region very slightly as confirmed by a computation taking into account all mixture effects (circles in Fig. 11). We conclude that the variation of the saturation temperature with composition change

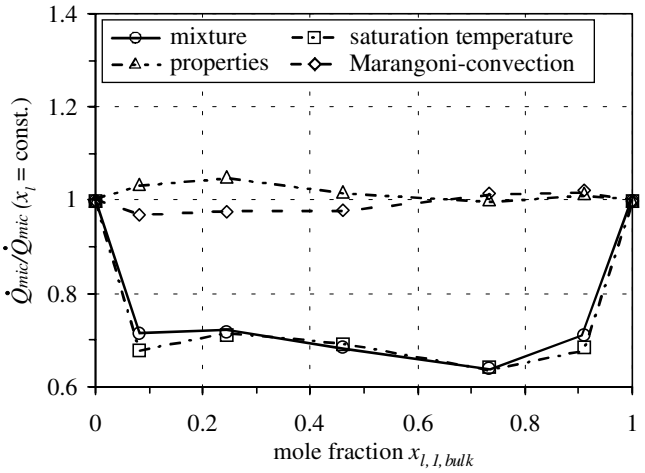

Fig. 11. Ratio of heat flow $\dot{Q}_{mic}$ considering selected effects and heat flow $\dot{Q}_{mic}$ (x_l = const.) assuming constant liquid composition in the micro-region of the binary mixture propane/*n*-butane, $p_r = 0.2$, $\dot{q}_m = 2 \times 10^4$ W/m^2, $r = d_{dep}/4$.

in the micro-region is quite important while the variation of properties and the Marangoni convection are almost negligible in the micro-region.

3.2. Macroscopic scale

In the macro region the models of Stephan and Hammer (1994) as well as Kern and Stephan (2000, 2003a,b) account for two-dimensional heat conduction within the thermal boundary layer and evaporation at the phase interface. In most industrial evaporators liquid evaporates on the outer surface of horizontal tubes. Due to bubbles sliding at the perimeter of the cylinder an additional enhanced convection takes place. Based on the model presented in Section 2, Mann and Stephan (2000b) adapted an additional model accounting for the convective terms. They computed for pure substances the contribution of free convection, evaporation, and forced convection to the overall heat transfer coefficient (Mann and Stephan, 2000b). As Fig. 12 shows, these contributions depend on the wall superheat ΔT. The pressure is also an important parameter. The authors calculated that the additional convective effects at tubes due to sliding bubbles can be significant.

Compared to pure substances the heat transfer coefficient is also a function of concentration (Fig. 6). Effects responsible for the characteristic reduction of binary mixture heat transfer coefficients have been identified by Kern and Stephan (2003b). They showed that the microscale mixture effects, as presented in the preceding section, the bubble site density, and the departure diameter explain the reduced heat transfer coefficient.

Thus from a macroscopic point of view bubble site density and departure diameter are governing parameters. In this study, four different cases were investigated. The cases are (symbols in brackets are also used in the following figures):

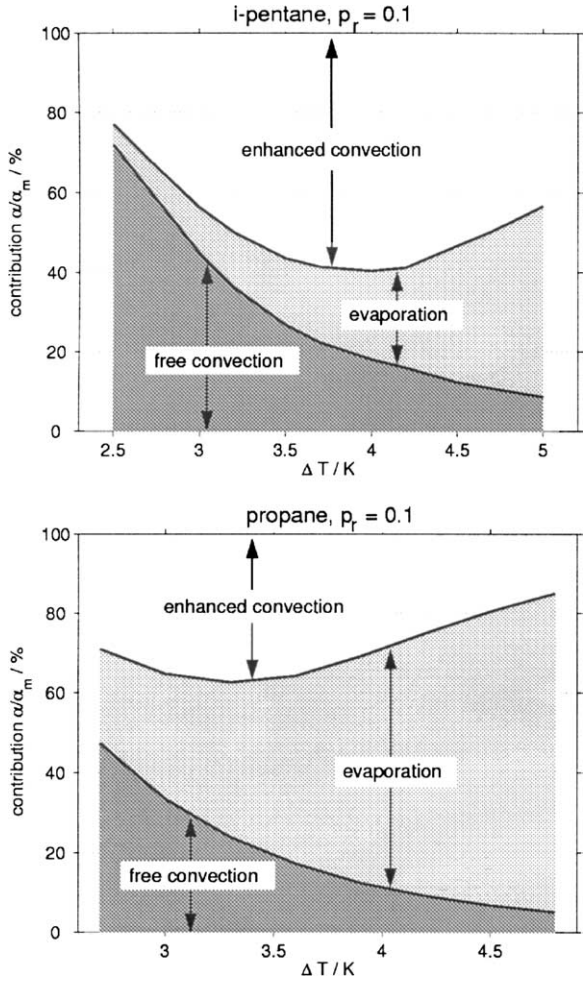

Fig. 12. Contribution of different heat transfer mechanisms to the overall heat transfer coefficient (Mann and Stephan, 2000b).

1. *Mixture* (○). Complete calculation considering all mixture effects.
2. *Pure* (□). Concentration in the micro-region is kept constant corresponding to the bulk mole fraction, i.e., all mixture effects in the micro-region are neglected.
3. *Ideal bubble site density* (△). Based on case 2 (“pure”), but using the ideal bubble site density (i.e., the molar average of the bubble site densities of the two pure components of the mixture) as input data for the model instead of the measured data at the bulk mole fraction.
4. *Ideal departure diameter* (◇). Based on case 3 (ideal bubble site density), but using the ideal departure diameter (i.e., the molar average of the departure diameters of the two pure components of the mixture) as input data for the model

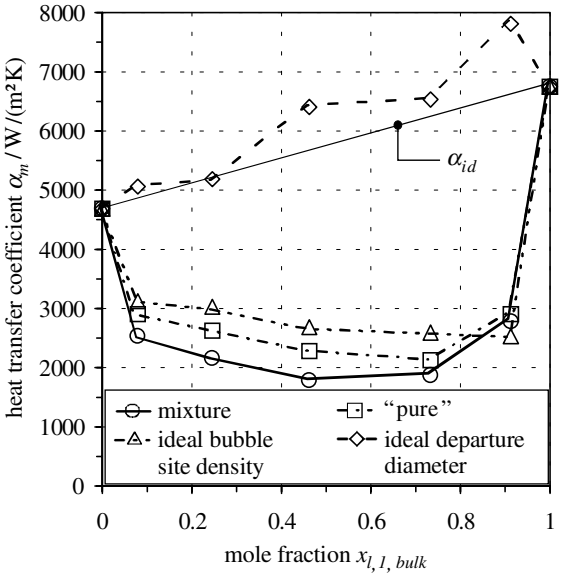

Fig. 13. Variation of decisive mixture effects. Calculated heat transfer coefficients of the binary mixture propane/nbutane for different compositions, $p_r = 0.2$, $\dot{q}_m = 2 \times 10^4$ W/m^2.

instead of the measured data at the bulk mole fraction.

In Fig. 13 computed heat transfer coefficients for propane/*n*-butane are plotted versus the liquid mole fraction of the bulk. The circles represent calculations with all mixture effects considered (case 1, ○ in Fig. 13). If the microscopic concentration gradients and the related effects are neglected, heat transfer coefficients are only slightly higher (case 2, □ in Fig. 13). As is well known from experiments, bubble site density and departure diameter of the mixture, that are still input data to the computation, clearly differ from the corresponding values of the two pure components of the mixture (Fig. 14). Introducing an ideal bubble site density and considering it as input parameter to the model, the calculated heat transfer coefficients are higher (case 3, △ in Fig. 13) compared to case 2. Considering additionally the ideal departure diameter (Fig. 14) as input parameter, the resulting heat transfer coefficients are in the range of the ideal heat transfer coefficient α_{id} (case 4, ◇ in Fig. 13). The ideal heat transfer coefficient is defined as the molar average of the heat transfer coefficients of the two pure components of the mixture. The parameter study indicates that the influence of microscale mixture effects is in this example of the same order as the influence of the bubble site density. Each of these two effects account for approx. 10% of the reduction of the heat transfer coefficient α_m compared to the ideal one α_{id}. The influence of the reduced departure diameter is rather large. It accounts for approx. 80% of the reduction of the heat transfer coefficient α_m.

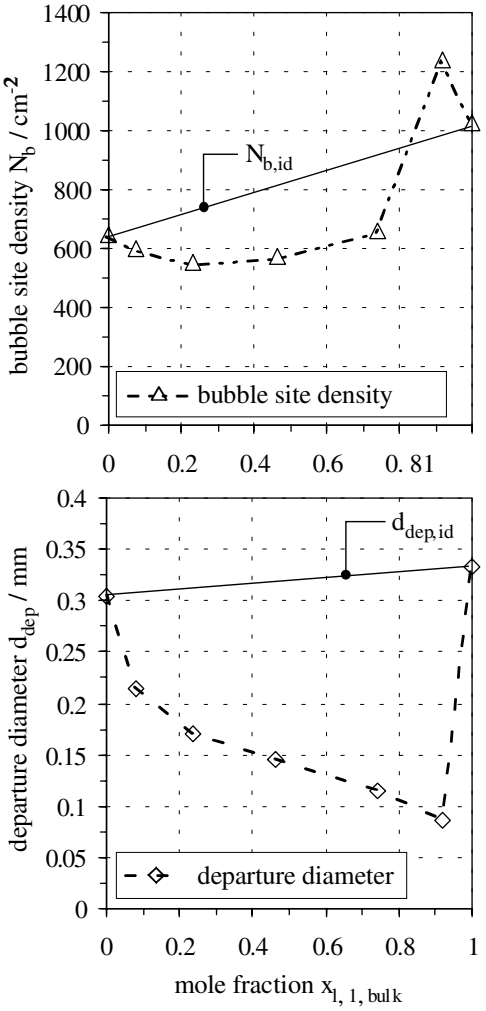

Fig. 14. Bubble site density and departure diameter of the binary mixture propane/*n*-butane for different compositions, $p_r = 0.2$, $\dot{q}_m = 2 \times 10^4$ W/m^2.

4. Conclusions

Nucleate boiling heat transfer can be well predicted using theoretical models including microscale heat and mass transfer.

On the microscale, heat transfer is governed by one-dimensional heat conduction normal to the wall, the molecular interfacial phase change resistance, and intermolecular forces of adsorption. Mass transfer is influenced by capillary forces and an evaporation induced flow. In a mixture composition changes due to the preferential evaporation of one component of the mixture and hence the liquid vapor phase equilibrium changes significantly. Further transport phenomena due to concentration gradients, e.g., diffusive mass transfer and Marangoni convection, are negligible on that scale. Micro-region results at the boundary to the macro-region imply that diffusive mass transfer in the macro-region is dominated by convective mass transfer.

On the macroscale, heat transfer is governed by transient heat conduction within the wall and the thermal boundary layer as well as evaporation at the phase interface of the vapor bubbles. For nucleate boiling on tubes additional convective effects due to sliding bubbles can have a significant influence on the heat transfer coefficient. The results of different investigations concerning the contribution of heat transfer during pinch-off to overall heat transfer is contradictory. Bae et al. (1999) reported a significantly contribution, while Mann and Stephan (2000a) obtained only a little influence from their numerical model. For binary mixtures two decisive parameters could be identified that are responsible for the characteristic reduction of heat transfer coefficients at intermediate compositions. These are bubble site density and departure diameter.

Acknowledgement

The authors are indebted to Deutsche Forschungsgemeinschaft, Bonn, for financial support.

References

Ammermann, C.N., You, S.M., Hong, Y.S., 1996. Identification of pool boiling heat transfer mechanisms from a wire immersed in saturated FC-72 using a single-photo/LDA method. ASME J. Heat Transfer 118, 117–123.

Bae, S., Kim, M., Kim, J., 1999. Improved technique to measure time- and space-resolved heat transfer under single bubbles during saturated pool boiling of FC-72. Exper. Heat Transfer 12, 265–278.

Bai, Q., Fujita, Y., 1999. Numerical simulation of the growth for a single bubble in nucleate boiling. Therm. Sci. Eng. 7, 45–53.

Barthau, G., 1992. Active nucleation site density and pool boiling heat transfer–an experimental study. Int. J. Heat Mass Transfer 35, 271–278.

Bednar, W., Bier, K., 1994. Wärmeübergang beim Blasensieden von binären Kohlenwasserstoffgemischen. Ph.D. Thesis, Fortschritt-Berichte VDI, 3 (357), VDI-Verlag, Düsseldorf.

Beer, H., 1971. Das dynamische Blasenwachstum beim Sieden von Flüssigkeiten an Heizflächen. Forsch. Ing.-Wes. 37, 85–90.

Dhir, V.K., 2001. Numerical simulations of pool-boiling heat transfer. AIChE J. 47 (4), 813–834.

Forster, H.K., Zuber, N., 1954. Growth of a vapor bubble in a supersaturated liquid. J. Appl. Phys. 25, 474.

Fujita, Y., Tsutsui, M., 1994. Heat transfer in nucleate pool boiling of binary mixtures. Int. J. Heat Mass Transfer 37, 291–304.

Hammer, J., 1996. Einfluß der Mikrozone auf den Wärmeübergang beim Blasensieden. Ph.D. Thesis, Fortschritt-Berichte, VDI, 19(96), VDI-Verlag, Düsseldorf.

Hammer, J., Stephan, P., 1995. Results of the micro-region model for nucleate boiling heat transfer. In: Proceedings 4th UK National Heat Transfer Conference, pp. 283–287.

Höhmann, C., Stephan, P., 2002. Microscale temperature measurement at an evaporating liquid meniscus. J. Exper. Therm. Fluid Sci. 26 (2-4), 157–162.

Hsu, Y.Y., Graham, R., 1961. An analytical and experimental study of the thermal boundary layer and ebullient cycle in nucleate boiling. NASA Report TN-D-594.

Judd, R.L., Hwang, K.S., 1976. A comprehensive model for nucleate pool boiling heat transfer including microlayer evaporation. ASME J. Heat Transfer 98, 623–629.

Kern, J., Stephan, P., 2000. Influence of microscale concentration gradients in nucleate boiling heat transfer of binary mixtures. Multiphase Sci. Technol. 12 (3-4), 233–247.

Kern, J., Stephan, P., 2003a. Theoretical model for nucleate boiling heat and mass transfer of binary mixtures. ASME J. Heat Transfer 125, 1106–1115.

Kern, J., Stephan, P., 2003b. Investigation of decisive mixture effects in nucleate boiling of binary mixtures using a theoretical model. ASME J. Heat Transfer 125, 1116–1122.

Krupiczka, R., Rotkegel, A., Ziobrowski, Z., 2000. The influence of mass transfer on the heat transfer coefficients during the boiling of multicomponent mixtures. Int. J. Therm. Sci. 39, 667–672.

Mann, M., Stephan, K., 2000a. Prediction of bubble departure diameters in nucleate boiling. In: Proceedings 3rd European Thermal Sciences Conference, vol. 2, pp. 749–754.

Mann, M., Stephan, K., 2000b. Influence of convection on nucleate boiling heat transfer around horizontal tubes. Multiphase Sci. Technol. 12 (3), 1–13.

Schlünder, E.U., 1986. Heat transfer in nucleate boiling of mixtures. In: Proceedings 8th International Heat Transfer Conference 4(4), pp. 2073–2079.

Stephan, K., Abdelsalam, M., 1980. Heat-transfer correlations for natural convection boiling. Int. J. Heat Mass Transfer 23, 73–87.

Stephan, P., Busse, C.A., 1992. Analysis of the heat transfer coefficient of grooved heat pipe evaporator walls. Int. J. Heat Mass Transfer 35, 383–391.

Stephan, P., Hammer, J., 1994. A new model for nucleate boiling heat transfer. Heat Mass Transfer 30, 119–125.

Stephan, P., Höhmann, C., Kern, J., 2002. Microscale measurement of wall-temperature distribution at a single vapor bubble for evaluation of a nucleate boiling model. Proceedings Space Technology and Applications International Forum, 163-171.

Stephan, K., Körner, M., 1969. Berechnung des Wärmeübergangs verdampfender binärer Flüssigkeitsgemische. Chem. Ing. Tech. 41, 409–416.

Wayner, P.C., Kao, Y.K., LaCroix, L.V., 1976. The interline heat transfer coefficient on an evaporating wetting film. Int. J. Heat Mass Transfer 19, 487–492.